# SERIES AND PARALLEL CONNECTION OF INDIVIDUAL Pd-MODIFIED ZnO NANOWIRES FOR GAS SENSING APPLICATIONS

**O. Lupan[1,2,3*], V. Postica[1], V. Cretu[1], T. Pauporte[3], and R. Adelung[2]**

*[1]Department of Microelectronics and Biomedical Engineering, Technical University of Moldova, Stefan cel Mare Av. 168, Chisinau, MD-2004 Republic of Moldova,*
*Email: oleg.lupan@mib.utm.md*
*[2]Faculty of Engineering, Institute for Materials Science, Christian-Albrechts Universität zu Kiel, Kaiser Str. 2, Kiel, D-24143 Germany*
*E-mail: ollu@tf.uni-kiel.de*
*[3]PSL Research University, Chimie ParisTech-CNRS, Institut de Recherche de Chimie Paris, UMR8247, 11 rue Pierre et Marie Curie, Paris, 75005 France*
*E-mail: thierry.pauporte@chimie-paristech.fr*

(Received September 5, 2016)

## Abstract

The hydrogen gas sensing properties of nanodevices based on two ZnO nanowires (NWs) functionalized/modified with palladium (Pd/ZnO) at room temperature are studied. The main goal of the study is to find which of the connections—in series or in parallel—is more favorable to improve the properties of a double NW nanodevice in comparison with a single Pd/ZnO NW-based nanosensor. An enhancement in gas response is observed in both cases. In the case of connection in series of two NWs, it is attributed to an increased number of Schottky barriers, which are directly related to sensor response to gases. In the case of parallel connection of two NWs, higher electrical currents can flow through the device; it improves the sensor response too; in addition, this type of device can be more easily integrated in electronics due to higher currents in passive regime (in air) and is more stable.

## 1. Introduction

The extraordinary properties of nanostructures are quite attractive for the development of novel analytical nanodevices that have advantages over traditional microelectronic devices, such as lower-cost, simpler design, higher performance, selectivity, and sensitivity [1, 2]. In the past decade, scientists have paid a lot of attention to the integration of semiconducting oxide into nanodevice applications, in particular, miniature gas sensors and biosensors [2–8]. Nanosensors exhibit the following main advantages.

(i) Compared to devices based on metal oxide nano- and microstructures which need a high operating temperature for efficient performance (150–500ºC) [9], the nanosensors based on individual nanostructures can operate properly even at room temperature [2, 3, 5, 6]. This feature eliminates the necessity to produce and integrate microheaters; as a consequence, it is possible to reduce the cost and power consumption of the final device [4]. There are publications that describe efficient gas detection at room temperature of individual nanostructures down to ppb

level [2, 6]. In addition, it provides the possibility of using organic materials as a sensing structure for sensor applications [10, 11].

(ii) Due to operation at room temperature, the physical and chemical properties of the sensing material (e.g., NWs, nanobelts) do not change over time [5]; this feature is strategically important for long-term stability of gas sensors [12].

(iii) Ultra-low power consumption in a passive state. Due to low currents that pass through a nanostructure, the power consumption of nanodevices is in the nW range [2–4]. Since portable devices, e.g., smartphones, are in a rapid progress and extensively used due to commodity and time saving, the necessity of low-power electronics has become of vital importance [4]. Thus, the development of nanoelectronic devices can solve this problem.

(iv) Possibility of fabricating miniature low-weight devices. Nanometer sizes of the sensitive material provide a possibility of designing nanoelectronic systems, such as an electronic nose (e-nose) with high yield [13]. This is very important for wearable sensors, biomedical and biological sensors for continuous monitoring of different human body biosignals (glucose, oxygen saturation, etc.) and quality of environment (fast detection of toxic gases, such as CO and $H_2S$, or highly inflammable gases, such as $H_2$). Another important example is photodetectors of ultraviolet (UV) light, especially UV-B ($\lambda$ = 280–315 nm), which can prevent risk factor of harmful effect of long exposure to dangerous sun rays.

In the past decades, miniaturization of electronic devices has been successfully implemented using "bottom–up" approaches, which have been extensively used to assembly semiconductor nanostructures into different devices, such as logic gates [14], gas sensors and biosensors [2, 15], photodetectors [4], etc. The next step of progress was combination and integration of several nanostructures in the same device; it has significantly extended the application domain [1, 14]. In the case of gas sensors, only comparison of gas sensing properties between single and multiple randomly oriented NWs has been reported [11, 16] and no comparison of series and parallel connected NWs has yet been made. Zhang *et al*. [6] have shown that multiple $In_2O_3$ NWs have higher reliability, sensitivity, and fabrication simplicity than those of single NWs. Khan *et al*. [16] have reported a higher gas response of multiple ZnO NWs compared to single NWs. In both cases, the effects can be related to the nanojunctions between NWs. The formed potential barriers in the nanojunctions are highly sensitive to gas species, and a higher modulation of device resistance can be obtained [16]. However, to date, there have been no reports on comparison of the gas sensing properties of NWs connected in parallel and series, which is very interesting from the fundamental point of view too. Insight into this idea can create a new paradigm in gas sensor science and engineering for fabrication of novel nanodevices with improved gas sensing properties and rational assembly/design of sensing devices.

In this study, we describe the gas sensing properties of nanodevices based on two Pd/ZnO NWs connected in series and parallel in order to find which of the connections is more favorable for improving the nanodevice performance in comparison with individual Pd/ZnO NWs (reported in Ref [17]). Our experimental results have shown that connection in series can significantly—about 2 times—improve the sensing properties of the nanodevice, while connection in parallel is less effective. The mechanism responsible for gas sensing of both types of devices has been discussed in detail. The enhancement in response in the case of connection in series can be attributed to an increased number of Schottky barriers (SBs).

## 2. Experimental

The Pd/ZnO NWs were grown by one-step electrochemical deposition (ECD) in a classical three-electrode electrochemical cell at 90 °C as described in Ref [17, 18]. The F-doped $SnO_2$ (FTO, 10 Ω/sq) films were used as substrates and as a working electrode for electrodepositon [17, 18]. The substrate cleaning procedure was described in Ref [17, 18]. The dependence of the morphological, structural, optical, and chemical properties on the concentration of the $PdCl_2$ solution added in the electrolyte solution was studied in detail in Ref [17]. TEM measurements showed the growth of Pd nanoparticles (NPs) onto the ZnO NW surface [17]. In addition, it was reported by Yang *et al*. [19] that Pd deposition occurs at high current efficiency and the process of Pd NP growth can be described by the following equation [19, 20]:

$$PdCl_4^{2-}(aq) + 2e^- \rightarrow Pd(s) + 4Cl^- \quad (1)$$

In this study, NWs from samples grown with the addition of 1 μM $PdCl_2$ (Alfa Aesar) into an electrolyte solution were examined. This concentration leads to a 0.6 at% Pd content in Pd/ZnO samples [17]. Morphological, structural, and chemical studies were performed by SEM, XRD and EDX techniques as described in [17, 18]. The gas sensing studies were conducted at room temperature at a 30% relative humidity as described in [3, 4]. Electrical measurements were continuously recorded using a Keithley 2400 source meter controlled through Lab View software (National Instruments). The nanosensor was prepared using a FIB/SEM system as described in Ref [3, 4]. All sensors exhibited a typical *n*-type behavior; that is, the resistance of the nanodevices decreased during exposure to $H_2$. Gas response ($S$) was defined as $S = R_{air}/R_{gas}$, where $R_{air}$ and $R_{gas}$ are the resistances of the nanodevice in air and under $H_2$.

## 3. Results and discussion

### *3.1. Characterization of Pd/ZnO NW arrays*

Figures 1a–1c show SEM images of Pd/ZnO NW arrays at different magnifications (from lower (Fig. 1a) to higher magnification (Fig. 1c)). The NWs are vertically aligned on an FTO substrate and show a homogenous and uniform coverage. The preferential anisotropic growth is known to result from differences in growth rates of the different crystal faces of ZnO, i.e., much higher growth rate of the (0001) surface than that of the $\{10\bar{1}0\}$ faces [21].

Details of pristine ZnO NW array morphology and the effect of various parameters of ECD can be found in Ref [18, 22]. The diameter ($D$) of NWs is in a range of 100–200 nm (measured using top view images, Fig. 1c), while the length ($L$) is in a range of 1–3 μm (from cross-sectional images, not shown here). The density of NWs is ≈10 NW/μm$^2$. Figure 1d shows the XRD pattern of the Pd/ZnO NW arrays recorded in a range of 10°–80° with a scanning step of 0.02°. All detected diffraction peaks can be attributed to the ZnO crystal phase with a hexagonal wurtzite structure (PDF#00-036-1451) and the $SnO_2$ crystal phase with a tetragonal structure (PDF#01-088-0297) originated from the FTO ($SnO_2$ : F) substrate [17, 18]. Peaks attributed to Pd, Pd-oxide phase (PdO), or impurities were not observed in the measured XRD spectra of investigated sample [12]. Higher intensity of the XRD peak corresponding to the (002)

plane (Fig. 1d) confirms SEM data on the preferential growth of NWs along the *c*-axis normal to the substrate (Figs. 1a–1c).

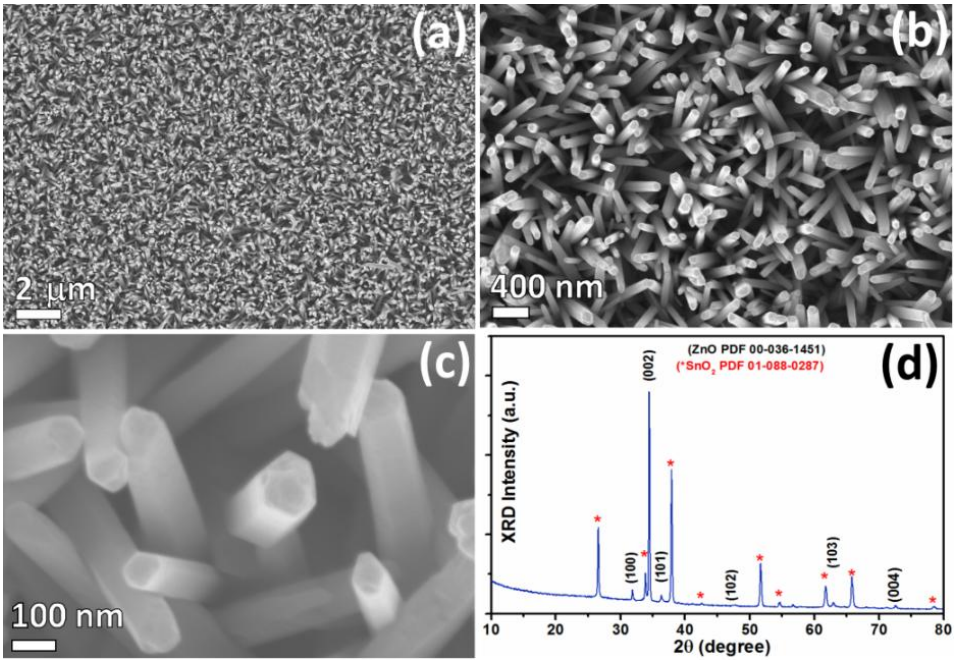


**Fig. 1.** (a–c) SEM images of Pd/ZnO nanowire arrays grown by ECD method on an FTO substrate at different magnifications (from low (a) to high (c)). (d) XRD spectrum of Pd/ZnO nanowire arrays and FTO ($SnO_2$ : F) substrate.

Figure 2 shows the EDX-line scan profile of Zn, O, and Pd taken along (Fig. 2b) and across (Fig. 2c) the Pd/ZnO NW agglomeration. It was observed that the Zn and O profiles properly follow the position of Pd/ZnO NWs, which is more clear in the case of line data 3 (Fig. 2c). However, due to the low content of Pd (0.6 at%) on the Pd/ZnO NWs surface, no detectable changes of Pd profile are observed (see Fig. 2).

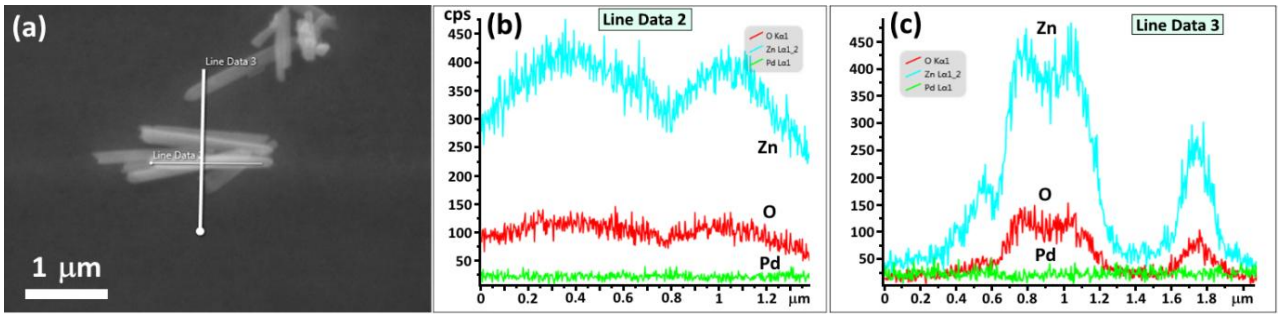


**Fig. 2.** (a) SEM image of EDX-scanned regions. EDX-line scan profile of Zn, O, and Pd taken: (b) along; and (c) across the Pd/ZnO NWs.

### *3.2. Series and parallel connection of individual Pd/ZnO NWs for nanodevices in gas sensing applications*

Figure 3a shows a device based on two Pd/ZnO NWs connected in series to pre-patterned Au pads of a $SiO_2$/Si chip by Pt contacts (Device 1). Each NW was designated as NW1 and NW2. The *D* and *L* values of both NWs are in the same range (diameter $D \approx 160$ nm and length $L \approx 1$ μm). Zoomed views of each of the NWs are shown in Figures 3b and 3c. The current–voltage curves show the formation of double Schottky contacts at the Pt/ZnO interfaces (Fig. 3d). Since electron affinity ($\chi$) of ZnO is 4.5 eV and the work function ($\phi_m$) of Pt is 6.1 eV, a SB at the Pt/ZnO interface was formed (Fig. 3e) [23]. Thus, the schematic structure of Device 1 connected to the measurement unit was represented in Fig. 3f, where $R_{NW1}$ and $R_{NW2}$ denote the resistance of NW1 and NW2, respectively, and Schottky diodes represents the SBs formed at the Pd/ZnO interface. Device2 consists of two Pd/ZnO NWs connected in parallel (see Fig. 3g). As in the case of Device1, the NWs are designated as NW1 and NW2. The *D* and *L* values of both NWs are in the same range ($D \approx 190$ nm and $L \approx 1.3$ μm). Zoomed views of each of the NWs are shown in Fig. 3h and Fig. 3i. The same double-Schottky characteristic was observed for Device2 (see Fig. 3j). The respective schematic structure of Device2 connected to the measurement unit is shown in Fig. 3k.

Next, the gas sensing studies of the fabricated devices (Devices 1 and 2) will be described. Figure 4a shows the gas response of a single NW nanosensor (curve *1*) and two individual Pd/ZnO NWs connected in series (curve 2) to 100 ppm $H_2$ gas at room temperature. All NWs integrated in the devices are from the same sample (SEM image for the device based on a single NW is not shown here) and have approximately the same geometrical dimensions ($D \approx 160 \pm 5$ nm and $L \approx 1 \pm 0.5$ μm). It is evident that the gas response increases about 2 times in the case of connection of two individual Pd/ZnO NWs in series compared to a single NW ($S \approx 105$ for a single NW and $S \approx 206$ for double NWs connected in series, see Fig. 4a). Only a slight difference in response time $\tau_r$ and recovery time $\tau_d$ (defined as necessary times for reaching and recovering 90% of full response, respectively) was observed. Thus, for the single NW, $\tau_r \approx 28$ s and $\tau_d \approx 31$ s, while for the NWs connected in series, $\tau_r \approx 24$ s and $\tau_d \approx 30$ s.

In the case of Device 2, an enhancement in gas response by about 1.3 times was obtained in the case of connection of two individual Pd/ZnO NWs in parallel compared to a single NW-based nanosensor ($S \approx 95$ for a single NW and $S \approx 120$ for NWs connected in series, see Fig. 4b). As in the case of connection in series (Device 1, Fig. 4a), the parallel NWs integrated in devices (Device 2, Fig. 4b) have approximately the same geometric dimensions ($D \approx 190 \pm 5$ nm and $L \approx 1.3 \pm 0.5$ μm). It is evident that the response and recovery times are not quite different and lie in a range of ≈20 s and ≈30 s, respectively (see Fig. 4b).

The sensitivity obtained for Device 1 and Device 2 is ≈200%/ppm and ≈120%/ppm, respectively. These values are lower than those reported for Pd/InP and Pd/$SiO_2$/AlGaN diode-based sensors [24, 25]; however, the metal–semiconductor–metal (double Schottky) structure described in this study can be more easily fabricated to the diode-based device reported previously (since the Ohmic contact is not needed and technological processing steps are reduced) [26, 27]. In addition, in the case of a double Schottky structure, it is not necessary to study the optimal reverse bias voltage for higher sensitivity, since it exhibits bi-directional sensing capabilities and is more suitable for long-term detection for reverse and forward applied bias voltages [26, 27]. Figure 5 shows the proposed mechanism of the SB height (SBH) variation

for the Pt/ZnO NW/Pt sensor structure (double Schottky) at equilibrium in vacuum (Fig. 5a), at an applied bias voltage in vacuum (Fig. 5b), during exposure to ambient air with adsorption of oxygen ions at the Pt/ZnO interface (Fig. 5c), and during exposure to hydrogen gas with the formation of a dipole layer at the Pt/ZnO interface (Fig. 5d).

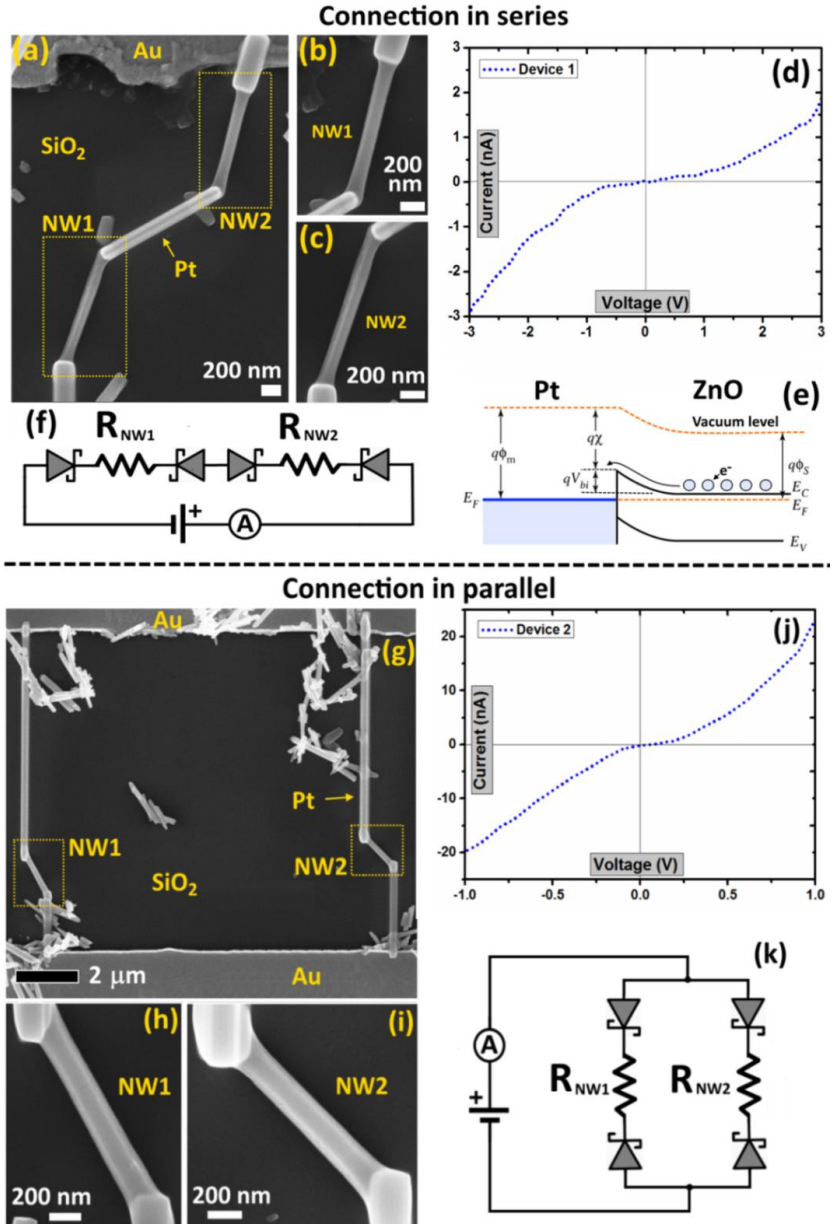


**Fig. 3.** (a) SEM image of Device 1 based on two Pd/ZnO NWs connected in series and zoomed-in regions of NW1 (b); and NW2 (c). (d) Current–voltage characteristic of Device 1 in the dark at room temperature. (e) Schematic structure of Device 1 connected to the measurement unit. (f) Energy band diagram of the Pt/ZnO contact. (g) SEM image of Device 2 based on two Pd/ZnO NWs connected in parallel and zoomed-in regions of NW1 (h); and NW2 (i). (j) Current–voltage characteristic of Device 2 in the dark at room temperature. (k) Schematic structure of Device 2 connected to the measurement unit.

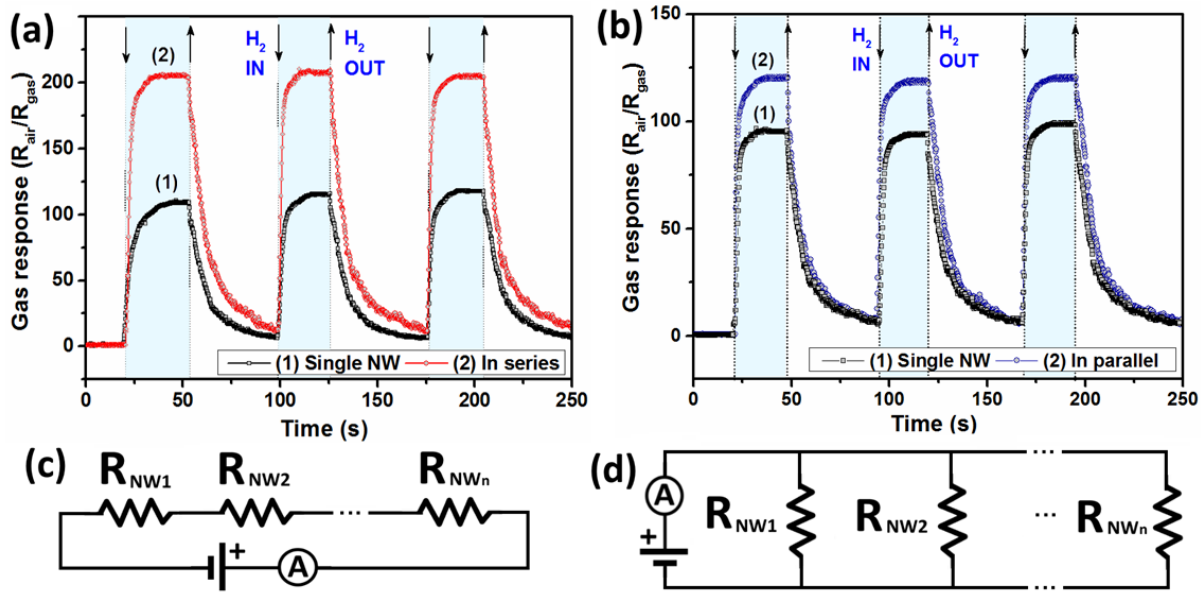


**Fig. 4.** (a) Gas response of a single NW and two Pd/ZnO NWs connected in series to 100 ppm $H_2$ gas (diameter $D \approx 160$ nm and length L ≈ 1 μm). (b) Gas response of a single NW and two Pd/ZnO NWs connected in parallel to 100 ppm $H_2$ gas ($D \approx 190$ nm and $L \approx 1.3$ μm). Schematics of the sensor structure based on individual Pd/ZnO NWs connected: (c) in series; and (d) in parallel.

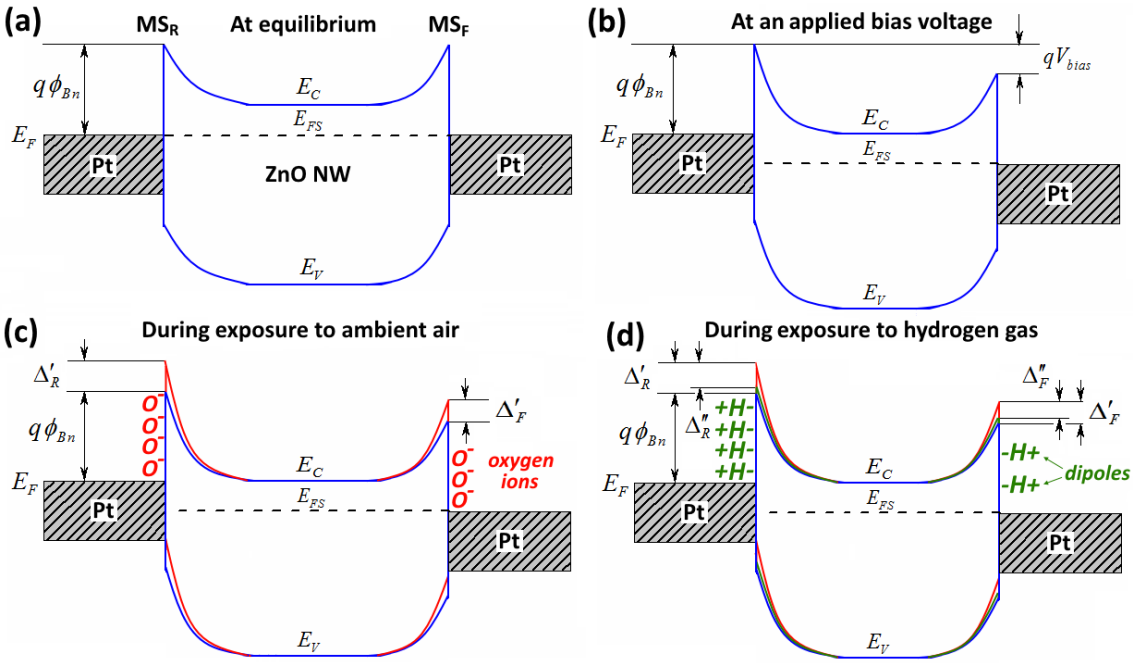


**Fig. 5**. Proposed mechanism of the SBH variation for the Pt/ZnO-NW/Pt sensor structure based on energy band diagrams: (a) at equilibrium in vacuum; (b) at an applied bias voltage in vacuum; (c) during exposure to ambient air with the adsorption of oxygen ions at the Pt/ZnO interface; and (d) during exposure to hydrogen gas with the formation of a dipole layer at the Pt/ZnO interface.

According to theoretical studies, the current density magnitude of the double Schottky structure at $V_{bias}$ is dominated by the metal/semiconductor contact at a reverse bias voltage ($MS_R$). Taking into account that the voltage drop across the metal/semiconductor contact at a forward bias ($MS_F$) is low and the voltage drop across the $MS_R$ is close to $V_{bias}$, the current density through the structure exposed to ambient air ($J_{air}$) can be expressed as follows [27, 28]:

$$J_{air} \approx A^* T^2 \exp\left(\frac{-\phi_{Bn} - \Delta'_R}{V_T}\right) \tag{2}$$

where $A^*$ is the Richardson's constant, $T$ is the absolute temperature, $\phi_{Bn}$ is the effective barrier height (EBH), $\Delta'_R$ is the change in EBH of $MS_R$ associated with the adsorption of oxygen species [28] and $V_T$ is the thermal voltage. In the case of exposure of the sensor structure to $H_2$ gas mixed with air, the current density magnitude ($J_{gas}$) is still determined by $MS_R$ [27, 28]:

$$J_{gas} \approx A^* T^2 \exp\left(\frac{-\phi_{Bn} - \Delta'_R + \Delta''_R}{V_T}\right) \tag{3}$$

where $\Delta''_R$ is the change in EBH induced by the dipole layer of $MS_R$ as a result of dissociation and diffusion of hydrogen molecules [27]. At a fixed temperature, the variation in SBH of $MS_R$ ($\Delta\phi_{BR}$) due to $H_2$ gas adsorption in the Schottky contact region can be expressed as follows [26, 29]:

$$\Delta\phi_{BR} = V_T \ln\left(\frac{J_{air}}{J_{gas}}\right) = V_p \ln\left(F\frac{[H_2]}{[H_2]_0}\right) \tag{4}$$

where $V_p$ is a fitting parameter, $F$ is an equilibrium constant associated with the $H^+$ ion coverage at the Pt/ZnO interface, $[H_2]$ is the $H_2$ gas concentration (in our case, 100 ppm), and $[H_2]_0$ is the intrinsic $H_2$ gas concentration in ambient air used for measurements (≈0.5 ppm) [26]. Accordingly, the sensor response can be expressed as follows [27]:

$$S = \frac{R_{air}}{R_{gas}} = \frac{J_{gas}}{J_{air}} = \exp\left(\frac{\Delta''}{V_T}\right) \tag{5}$$

The role of Pd NPs in the improvement of hydrogen gas sensing abilities was discussed in previous work [17]; it was attributed to an electrical sensitization mechanism (formation of a space charge region around the Pd, i.e., nano-SBs that narrow the conduction channel) and chemical sensitization mechanism (catalytic dissociation of molecular oxygen by Pd NPs, i.e., "spillover effect" which contributes to electron withdrawal from the ZnO NW) [30, 31]. Such properties of Pd as work function and conductivity are known to be efficiently modulated by the adsorption of $H_2$ gas. For details, see [17].

Next, the main causes of gas response enhancement in the case of series and parallel connection of two individual Pd/ZnO NWs will be analyzed. First, consider the case where SBs are excluded from the electrical circuit; that is, Ohmic contacts are formed at both ends of NWs. Since the nanostructures have approximately equal geometric dimensions in the two cases, on the assumption that $n$ NWs are connected in series (see Fig. 4c), the following condition can be true: $R_{NW1(air)} \approx R_{NW2(air)} \approx \ldots \approx R_{NWn(air)}$ and $R_{NW1(gas)} \approx R_{NW2(gas)} \approx \ldots \approx R_{NWn(gas)}$, where $R_{NW(air)}$ and $R_{NW(gas)}$ are the resistances of NWs exposed to the air and $H_2$ gas, respectively. Thus, in the case

of series connection, the total resistance of the device exposed to the air ($R_{T(air),series}$) and $H_2$ gas ($R_{T(air),series}$) is as follows [32]:

$$R_{T(air),parallel} = \sum_{i=1}^{n} R_{NWi(air)} = nR_{NW(air)} \tag{6}$$

$$R_{T(gas),parallel} = \sum_{i=1}^{n} R_{NWi(gas)} = nR_{NW(gas)} \tag{7}$$

Hence, the gas response can be defined as follows [32]:

$$S = \frac{R_{T(air),series}}{R_{T(gas),series}} = \frac{R_{NW(air)}}{R_{NW(gas)}} \tag{8}$$

In the case of connection in parallel, on the assumption that *n* NWs are connected in parallel (see Fig. 4d), the total resistance of the device exposed to the air ($R_{T(air),parallel}$) and $H_2$ gas ($R_{T(gas),parallel}$) is as follows [32]:

$$\frac{1}{R_{T(air),series}} = \sum_{i=1}^{n} \frac{1}{R_{NWi(air)}} = \frac{1}{R_{NW(air)}} \cdot n \tag{9}$$

$$\frac{1}{R_{T(gas),series}} = \sum_{i=1}^{n} \frac{1}{R_{NWi(gas)}} = \frac{1}{R_{NW(gas)}} \cdot n \tag{10}$$

hence, the gas response can be defined as follows [32]:

$$S = \frac{R_{T(air),parallel}}{R_{T(gas),parallel}} = \frac{R_{NW(air)}}{R_{NW(gas)}} \tag{11}$$

In conclusion, the addition of *n* number of NWs in series or parallel does not lead to a significant enhancement in gas response; it is equal to the *S* value of a single NW. Thus, it is reasonable to expect that the enhanced response of connected NWs is due to the increased number of SBs, especially in the case of connection in series. Hu *et al*. showed that the formed SB to a single nanostructure can considerably increase gas response due to the higher sensitivity of the SBH ($\phi_{bi}$) to adsorbed species in the Schottky contact region [15]. In addition, Katoch *et al*. [9] showed that a higher number of gas sensitive barriers in a nanomaterial enhance the gas response. Thus, we can speculate that, in our case, the enhanced response is attributed to an additional SB in series from the second NW.

However, in the case of connection in parallel, the SBs of NWs are in parallel and the number of SBs is the same in the two branches of current flow; thus, the slightly enhanced gas response can be attributed to another factor. Bai *et al*. [33] and Liu *et al*. [34] showed that an increased number of parallel ZnO NWs increase the detected photocurrent due to the increased number of channels for current flow. Thus, we believe that, in our case, for connection in parallel, the slight increase in gas response is due to possibility of higher current flow [34]. Further research is in progress.

## 4. Conclusions

The devices based on two individual Pd/ZnO NWs connected in series or in parallel have been successfully prepared using the Pt-deposition function of FIB/SEM scientific instrument and studied for gas sensing applications. An enhancement in gas response has been obtained in both cases. In the case of series connection of two Pd/ZnO NWs, the gas response has increased about two times, while in the case of connection in parallel, the gas response has increased only about 1.3 times. Thus, we can conclude that series connection is more efficient and better sensor performances are related to an increased number of SBs in the branch of current flow which are highly sensitive to adsorbed species in the contact regions. Thus, the described connection of nanostructures in series can be proposed as a promising method for rational fabrication of sensor devices with improved sensing properties.

**Acknowledgments.** The authors acknowledge professor dr. hab. Ion Tiginyanu, Institute of Electronic Engineering and Nanotechnologies, Academy of Sciences of Moldova, for discussions. The authors acknowledge the support from German Research Foundation (DFG) under scheme AD 183/12-1. This research was partly supported by project Institutional 45inst-15.817.02.29A funded by the Government of the Republic of Moldova and by the STCU within Grant 5989 at the Technical University of Moldova.

## References

[1] Y. Cui and C.M. Lieber, Science 291, 851, (2001).
[2] Y. Cui, Q. Wei, H. Park, and C.M. Lieber, Science 293, 1289, (2001).
[3] O. Lupan, G. Chai, and L. Chow, Microelectron. Eng. 85, 2220, (2008).
[4] O. Lupan, V. Cretu, V. Postica, M. Ahmadi, B.R. Cuenya, L. Chow, I. Tiginyanu, B. Viana, T. Pauporté, and R. Adelung, Sens. Actuators B 223, 893, (2016).
[5] O. Lupan, V.V. Ursaki, G. Chai, L. Chow, G.A. Emelchenko, I.M. Tiginyanu, A.N. Gruzintsev, and A.N. Redkin, Sens. Actuators B 144, 56, (2010).
[6] D. Zhang, Z. Liu, C. Li, T. Tang, X. Liu, S. Han, B. Lei, and C. Zhou, Nano Lett. 4, 1919, (2004).
[7] O. Lupan, G. Chai, and L. Chow, Microelectron. J. 38, 1211, (2007).
[8] T. Shishiyanu, O. Lupan, L. Chow, S. Shishiyanu, and S. Railean, Mold. J. Phys. Sci. 7, 42, (2008).
[9] A. Katoch, Z.U. Abideen, H.W. Kim, and S.S. Kim, ACS Appl. Mater. Interfaces 8, 2486, (2016).
[10] Y.S. Jung, W. Jung, H.L. Tuller, and C.A. Ross, Nano Lett. 8, 3776, (2008).
[11] H.-H. Lu, C.-Y. Lin, T.-C. Hsiao, Y.-Y. Fang, K.-C. Ho, D. Yang, C.-K. Lee, S.-M. Hsu, and C.-W. Lin, Anal. Chim. Acta 640, 68 ,(2009).
[12] V. Postica, I. Hölken, V. Schneider, V. Kaidas, O. Polonskyi, V. Cretu, I. Tiginyanu, F. Faupel, R. Adelung, and O. Lupan, Mater. Sci. Semicon. Proc. 49, 20, (2016).
[13] F. Röck, N. Barsan, and U. Weimar, Chem. Rev. 108, 705, (2008).
[14] Y. Huang, X. Duan, Y. Cui, L.J. Lauhon, K.-H. Kim, and C.M. Lieber, Science 294, 1313, (2001).
[15] Y. Hu, J. Zhou, P.-H. Yeh, Z. Li, T.-Y. Wei, and Z.L. Wang, Adv. Mater 22, 3327, (2010).

[16] R. Khan, H.W. Ra, J.T. Kim, W.S. Jang, D. Sharma, and Y.H. Im, Sens. Actuators B 150, 389, (2010).
[17] O. Lupan, V. Postica, T. Pauporté, and R. Adelung, Sens. Actuators B in progres, (2017).
[18] T. Pauporté, O. Lupan, J. Zhang, T. Tugsuz, I. Ciofini, F. Labat, and B. Viana, ACS Appl. Mater. Interfaces 7, 11871, (2015).
[19] F. Yang, S.-C. Kung, M. Cheng, J.C. Hemminger, and R.M. Penner, ACS Nano 4, 5233, (2010).
[20] Y. Xiong, J. Chen, B. Wiley, Y. Xia, Y. Yin, and Z.-Y. Li, Nano Lett. 5, 1237, (2005).
[21] J.B. Baxter, A.M. Walker, K.v. Ommering, and E.S. Aydil, Nanotech. 17, S304, (2006).
[22] O. Lupan, T. Pauporté, B. Viana, P. Aschehoug, M. Ahmadi, B.R. Cuenya, Y. Rudzevich, Y. Lin,and L. Chow, Appl. Surf. Sci. 282, 782, (2013).
[23] Z.L. Wang and J. Song, Science 312, 242, (2006).
[24] Y.-I. Chou, C.-M. Chen, W.-C. Liu, and H.-I. Chen, IEEE Electron Device Lett. 26, 62, (2005).
[25] C.-F. Chang, T.-H. Tsai, H.-I. Chen, K.-W. Lin, T.-P. Chen, L.-Y. Chen, Y.-C. Liu, and W.-C. Liu, Electrochem. Commun. 11, 65, (2009).
[26] K. Skucha, Z. Fan, K. Jeon, A. Javey, and B. Boser, Sens. Actuators B 145, 232, (2010).
[27] S.-Y. Chiu, H.-W. Huang, T.-H. Huang, K.-C. Liang, K.-P. Liu, J.-H. Tsai, and W.-S. Lour, Int. J. Hydrogen Energy 34, 5604, (2009).
[28] T.-Y. Wei, P.-H. Yeh, S.-Y. Lu, and Z.L. Wang, J. Am. Chem. Soc. 131, 17690, (2009).
[29] Y.M. Wong, W.P. Kang, J.L. Davidson, A. Wisitsora-at, and K.L. Soh, Sens. Actuators B 93, 327, (2003).
[30] N. Yamazoe, Sens. Actuators B 5, 7, (1991).
[31] A. Kolmakov, D.O. Klenov, Y. Lilach, S. Stemmer, and M. Moskovits, Nano Lett. 5, 667, (2005).
[32] P. Scherz, Practical electronics for inventors, McGraw-Hill, Inc.; 2006.
[33] S. Bai, W. Wu, Y. Qin, N. Cui, D.J. Bayerl, and X. Wang, Adv. Funct. Mater. 21, 4464, (2011).
[34] X. Liu, L. Gu, Q. Zhang, J. Wu, Y. Long, and Z. Fan, Nature Commun, 5, (2014).